Acceleron Aerospace Journal || AAJ.11.2106-2530
Volume 4, Issue 5, pp (1156-1164)
Research Paper
E-ISSN- 2583-9942 || DOI: 10.61359/11.2106-2530

Laser Beam Apparatus for Flow Visualization

Top David Thiec[*], Trinos Gama[†], Lencho Dereje Futassa[‡], Komborerai[§], Brandon[**]

and

Dharmander Singh Chand [††]

Department of Aerospace Engineering, Chandigarh University, Chandigarh, India.

Abstract: The laser beam apparatus for flow visualization technique is designed for advancements in fields like fluid dynamics through different enhanced flow visualization techniques as presented in this paper. The use of a powered laser source in conjunction with smoke allows for the possibility of observing and analyzing the fluid flow patterns over the body. The smoke acts as tracer particles for determining the flow patterns including laminar, turbulent and transitional behaviours. During this study, a combination of three approaches was used to reach the final comparison stage of the results, which are analytical, computational and experimental approaches. We investigated the flow of the fluid as it passes over a NACA 0012 airfoil in a custom-built wind tunnel. A low percentage error of 9.59% was obtained between the analytical and the experimental velocities. The results obtained accurately validate the apparatus setup effectiveness in representing the flow phenomena and giving further in-sights as to the interactions of boundary layers along with vortex formations. This study does not just suggest that the apparatus is capable for research and educational setting but also possess some potential applications in aerospace engineering, automotives design and environmental fluid studies.

Table of Contents

1. Introduction

Flow visualization has been crucial in different engineering fields like aerospace and automobiles. It enables engineers to identify the pattern of flow, the nature of interaction flow and solid surface and, hence analysing the results. There are various techniques of flow visualization which might categorized as either tracer based or density based. In the former technique, tracer such as dye and smoke are introduced to the flow, and their movement is observed to analyse the behaviour of the flow. Laser sheet and surface oil are few examples of this type. While the latter one relies on the change in reflective index caused by density change of the flow. It is helpful in shock visualization and heat transfer. Schlieren and shadowgraph techniques are of this type. In this work laser beam, for illumination, and smoke as tracer are integrated to visualize flow over a model of NACA0012 airfoil inside the subsonic wind tunnel for experimental purpose, and the same model underwent computational analysis by using ANSYS software to ensure the accuracy and reliability of the work. The aim of this work is to visualize flow to study both qualitative quality such as high-resolution visibility of pattern, boundary layer and quantitative quality such as velocity, vorticity, and turbulence of flow over the airfoil in subsonic wind tunnel with the integration of smoke as tracer and laser beam as illumination source for better results.

[*] Department of Aerospace Engineering, Chandigarh University, Chandigarh, India.
Corresponding Author: 21bas1307@cuchd.in.
[†] Department of Aerospace Engineering, Chandigarh University, Chandigarh, India.
[‡] Department of Aerospace Engineering, Chandigarh University, Chandigarh, India.
[§] Department of Aerospace Engineering, Chandigarh University, Chandigarh, India.
[**] Department of Aerospace Engineering, Chandigarh University, Chandigarh, India.
[††] Department of Aerospace Engineering, Chandigarh University, Chandigarh, India.
** Received: 17-April-2025 || Revised: 28-Mays-2025 || Accepted: 30-May-2025 || Published Online: 30-May-2025.

2. Literature Review

Flow visualization can be done in many different methods such as water channel, wind tunnel water, wind tunnel oil and particle image velocity [8]. These methods vary in their result visibility, cost effectiveness, and ease of experimental procedures. Not only smoke seeding but also the smoke wire technique has been used for visualizing flow especially in structures around drag driven turbines, where nichrome wire coated with safe oil illustrates the streamlines at varying airflow speeds [4]. While the above-mentioned techniques including water channel, wind tunnel water, and wind tunnel oil are cost effective and easy, their results are not optimized and hence the introduction of laser beam visualization and smoke is needed. To mention few, the laser light sheet flow visualization systems for a large-scale, low speed wind tunnel aimed at complement force and pressure data is used in visualizing off-body aerodynamic phenomena [10]. This technique can use smoke as flow tracers in large wind tunnels and others experimental apparatus suitable for it [11]. The most fascinating thing about laser-smoke flow visualization is that its applications are diverse. This is because it can be integrated into apparatus easily, gives clear results especially in the study of vortex formation over airfoil, cylindrical, and conical bodies [7].

Researchers explored the idea of integrating smoke-laser visualization with CFD, creating a robust hybrid technique that uses the strengths of each respective method resulting in optimized aerodynamic efficiency. Efforts have been made to develop robust quantitative methods such as an optical field measurement technique particularly for measuring scalar concentration fields using Mie scattering from smoke particles. New small-scale wind tunnels have been designed specifically for flow visualization, incorporating mini smoke generators and varied parameters such as honeycomb screens and illumination systems to enhance the visibility of smoke lines [31]. Also, the development of smaller wind-tunnels specifically for flow visualization allows for easier adaptation in diverse research groups with varying focuses such as automotive and universities.

Optical methods have been the most reliable in terms of accuracy and detail of flow observations. This is a result of consistent research in the field, which will be briefed below. There is a technique called Planar Laser Rayleigh Scattering; researchers make use of nanocrystals to capture detailed cross-sectional flow visualizations in supersonic wind tunnels. It is effective in identifying boundary-layer characteristics and flow asymmetries [33]. Non-Optical methods exist too, such as the use of Tufts and Oil Flow. These concepts on a fundamental level are placement of tufts or oil on the surface of a model in the test-section to clearly visualize flow direction and locating or identifying separation points. Future research may focus on enhancing these aspects to improve the accuracy and detail of flow visualizations. A combination of non-optical visualization techniques with computational fluid dynamics (CFD) has proven to provide a more comprehensive understanding of flow phenomena. This integration has immense potential, and its interdisciplinary nature is attractive and may inspire further innovation in wind tunnel techniques [38] [39].

3. Methodology

Experimental Methodology

Material Selection

The process of material selection in the experimental study of flow visualization is a very crucial process that encourages optimal performance, accurate data retained, durability and other important aspects of any setup. The general properties considered in the selection of laser source include wavelength, power and beam quality. The wavelength affects the flow pattern in terms of visibility. The power of the laser source is another important parameter that has to be considered because it affects the bright-ness of the laser and visibility of the beam as it illuminates the test section over the airfoil being tested. On the account of beam quality, it affects the focus ability and di-vergence of the laser beam. Some of the optical properties that have to be considered include lens material, focal length and aperture. The effect due to material of the lens is on the transmission and reflection of the laser beam. The laser beam is trans-mitted through the lens to the test section for illumination; thus, the material of the lens has to be properly selected for optimal transmission. The size and thickness of the laser sheet is affected but the focal length. The thickness of the laser sheet is inversely proportion-al to the focal length, which means that an increase in focal length reduces the thick-ness of the laser sheet and vice-versa. The aperture affects the amount of light that enters the optical system. A larger aperture allows more light to enter but may also increase the size of the optical system. The figure below illustrates the equipment used for experiments.

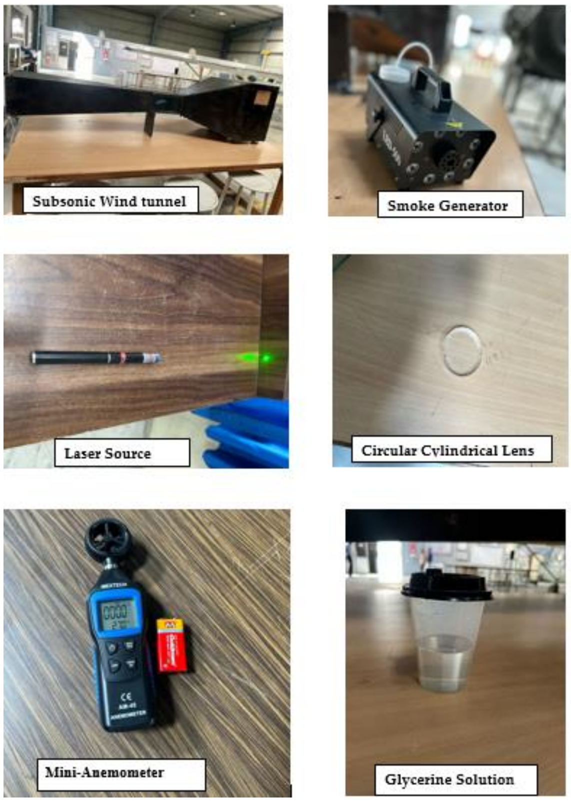

Figure 1: Equipment used in experiment

Experimental Procedure

- Setup the experiment by connecting the fan and smoke generator to the power source.
- Make sure that the airfoil is properly attached to the appropriate angle of at-tack.
- Pour the glycerin solution in the tank of the smoke generator.
- Switch on the smoke generator and wait for it to switch on the red light showing that is has heated up.
- Close the sides of the gazebo to make the test section dark
- Switch on the suction fan attached to the outlet of the wind tunnel.
- Measure the velocity of the flow inside the test section using a mini-anemometer
- When the smoke generator has heated up, press the button to release the smoke into the test section of the wind tunnel.
- Periodically start and stop the flow of the smoke in order to properly capture the attachment and detachment of the flow as it passes over the airfoil.
- Use a high-resolution camera to capture the pictures and videos of the flow as it passes over the airfoil.
- Repeat the procedure in order to obtain the most accurate results
- Switch of the smoke generator and the suction fan after the experiment is successfully completed.

Computational Methodology

Modelling, Meshing and Setup.

The computational analysis was done in such way that the wind tunnel test section with an airfoil (NACA0012) in it was modelled and simulated using ANSYS software. The model was attached to one of the walls at 00 angle of attack. The geometry was modelled using ANSYS space claim with the specifications of test section and the model. The length, width and depth for the test section are 12.40, 5.37 and 3.72m respectively whereas the chord length and span of the airfoil are 1 and 1.32m. Additionally, the test section was divided into two separate domains (Inner domain of 4×4×1.66m) in order to focus on the vicinity around the airfoil hence getting better results as shown in Figure 2.

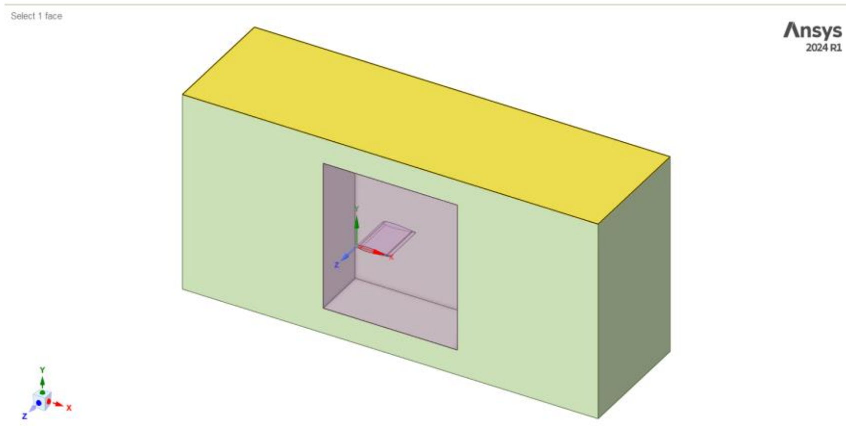

Figure 2: Model of an airfoil inside the test Section

For meshing, the tetrahedron method of meshing was chosen since a complex geometry i.e. a wing with a curving leading edge was present. Furthermore, the mesh metrics quality for the orthogonality and skewness were found to be 0.76 and 0.23 respectively, which verify the mesh to be of good quality. The mesh was made coarse in the outer domain of the test section and finer in the region of interest as seen in Figure 2. Additionally, an inflation was introduced around the wing area to capture boundary layer effects and interaction with wing walls.

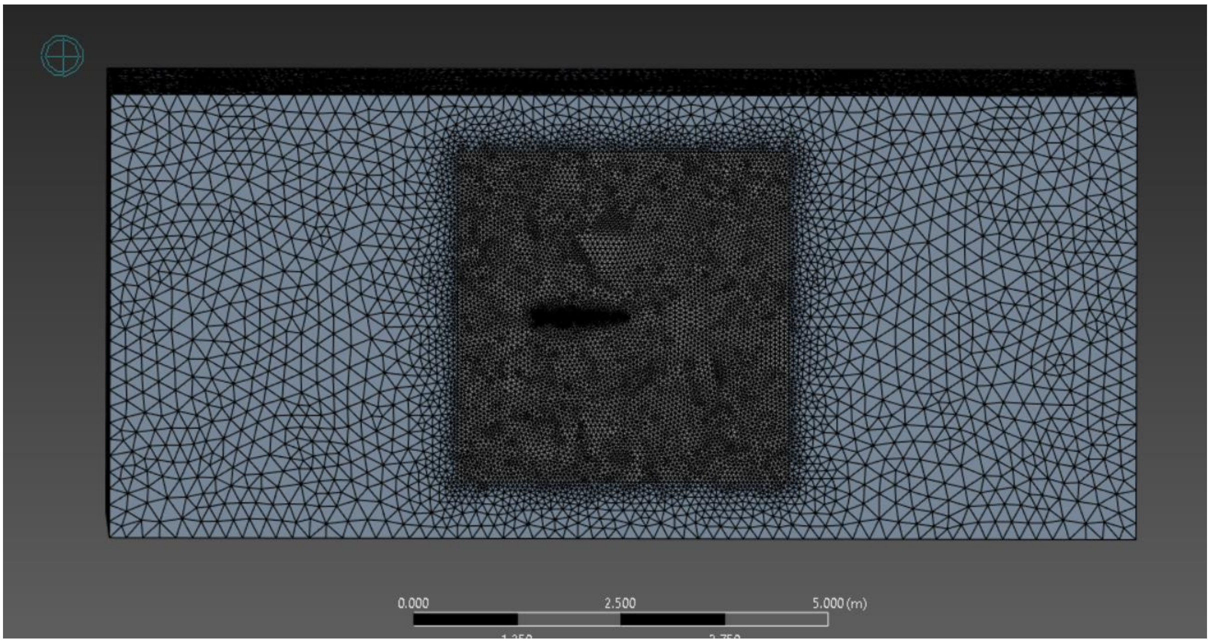

Figure 3: Mesh of the model

In the setup of the simulation, pressure-based solver type was used. The viscous model picked was a realizable k-epsilon model with non-equilibrium wall function. This is because the approach captures boundary layer effects in incompressible flow and targets the turbulence close to the wall of the wing model. For the boundary conditions, the velocity at the inlet was specified in components to account for the angle of attack while maintaining the wing model at zero degrees Angle of Attack (AOA) position. Suitably, Green-Gauss node based was opted for Spatial Discretization Gradient because the mesh used was unstructured type.

Governing Equations of the Ansys Fluent Simulation software.

This software is based on the governing equations of fluid dynamics which include mass, momentum and energy conservation equations. These equations are combined and are referred to as the Navier Stoke's equation.

Continuity equations

$$\frac{\partial \rho}{\partial t} + \nabla \cdot \left(\rho \vec{V}\right) = 0 \tag{3.1}$$

Momentum equation.

x-component

$$\frac{\partial(\rho u)}{\partial t} + \nabla \cdot (\rho u \vec{V}) = -\frac{\partial P}{\partial x} + \frac{\partial \tau_{xx}}{\partial x} + \frac{\partial \tau_{yx}}{\partial y} + \frac{\partial \tau_{zx}}{\partial z} + \rho f_x \tag{3.2}$$

y-component

$$\frac{\partial(\rho v)}{\partial t} + \nabla \cdot (\rho v \vec{V}) = -\frac{\partial P}{\partial y} + \frac{\partial \tau_{xy}}{\partial x} + \frac{\partial \tau_{yy}}{\partial y} + \frac{\partial \tau_{zy}}{\partial z} + \rho f_y \tag{3.3}$$

z-component

$$\frac{\partial(\rho \omega)}{\partial t} + \nabla \cdot (\rho \omega \vec{V}) = -\frac{\partial P}{\partial z} + \frac{\partial \tau_{xz}}{\partial x} + \frac{\partial \tau_{yz}}{\partial y} + \frac{\partial \tau_{zz}}{\partial z} + \rho f_z \tag{3.4}$$

Energy equation

$$\begin{aligned} \frac{\partial}{\partial t}\left[\rho\left(e + \frac{V^2}{2}\right)\right] + \nabla \cdot \left[\rho\left(e + \frac{V^2}{2}\vec{V}\right)\right] &= \rho \dot{q} + \frac{\partial}{\partial x}\left(k\frac{\partial T}{\partial x}\right) + \frac{\partial}{\partial y}\left(k\frac{\partial T}{\partial y}\right) + \frac{\partial}{\partial z}\left(k\frac{\partial T}{\partial z}\right) - \frac{\partial(up)}{\partial x} - \frac{\partial(vp)}{\partial y} - \frac{\partial(\omega p)}{\partial z} + \frac{\partial(u\tau_{xx})}{\partial x} \\ &+ \frac{\partial(u\tau_{yx})}{\partial y} + \frac{\partial(u\tau_{zx})}{\partial z} + \frac{\partial(v\tau_{xy})}{\partial x} + \frac{\partial(v\tau_{yy})}{\partial y} + \frac{\partial(v\tau_{zy})}{\partial z} + \frac{\partial(\omega\tau_{xz})}{\partial x} + \frac{\partial(\omega\tau_{yz})}{\partial y} \\ &+ \frac{\partial(\omega\tau_{zz})}{\partial z} + \rho\vec{f} \cdot \vec{V} \end{aligned} \tag{3.5}$$

Analytical Methodology.

The apparatus constructed required validation and evaluation of its accuracy. For that case, velocity at the test section is determined analytically and experimentally then compared, taking the analytical value as the reference. On the specifications of the suction fan, air delivery was given, which was used for calculation of the test section velocity by use of the conservation of mass flow.

4. Results and Discussion

Computational Results

The velocity vectors of the wing section at all the AOAs indicate zero velocity at the wall accounting for no slip condition. The velocity then gradually increases moving further in the perpendicular direction to the wall until the equivalent velocity to that at the test section is achieved. This can be seen clearly in Figure 4, where a U velocity profile is formed. Furthermore, at 5,10 and15 degrees AOA, it can be observed that there are points with reverse flow of fluid on the upper wing surface. This indicates boundary layer points of separation.

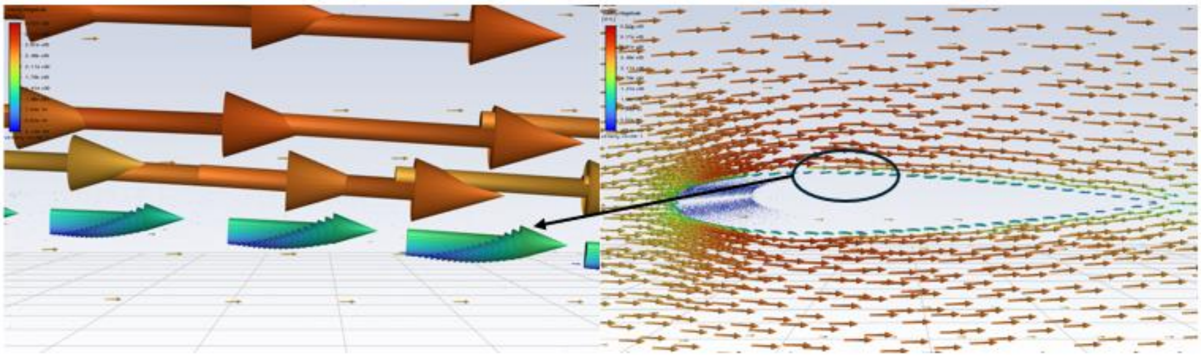

Figure 1: Zoomed in Velocity vector showing velocity profile at 0° AOA

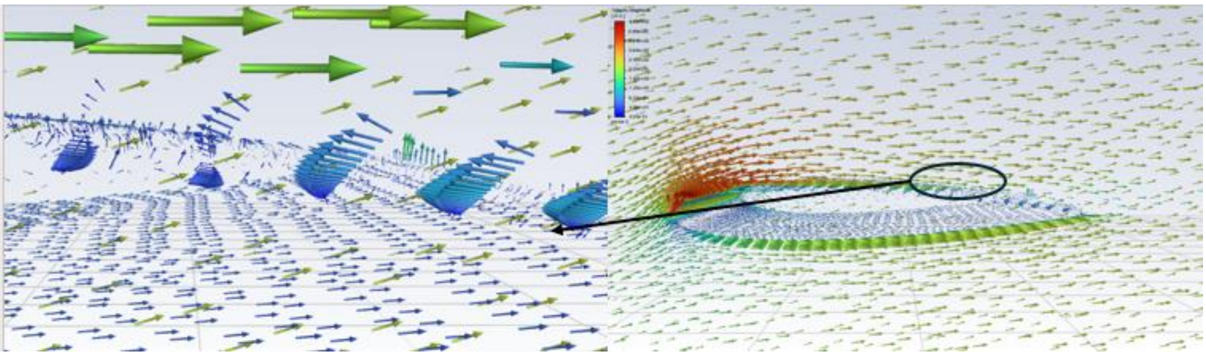

Figure 2:Zoomed in Velocity vector showing reverse flow at 5°AOA.

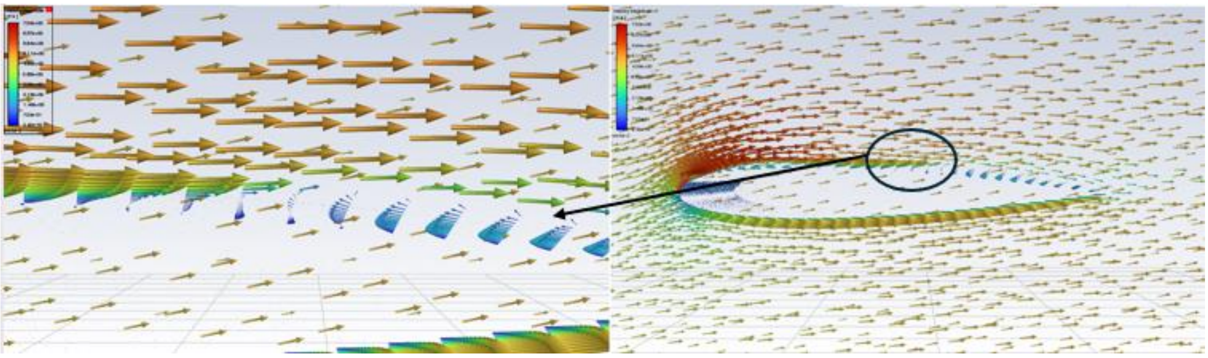

Figure 3:Zoomed in Velocity vector showing reverse flow at 10°AOA

Form Figure 5 and Figure 6, the reverse flow at the upper surface of the wing, at 10°AOA, starts at a point upstream closer to the leading edge as compared to that of 5°AOA. This means the separation of boundary layer happens earlier at 10°AOA than 5°AOA.

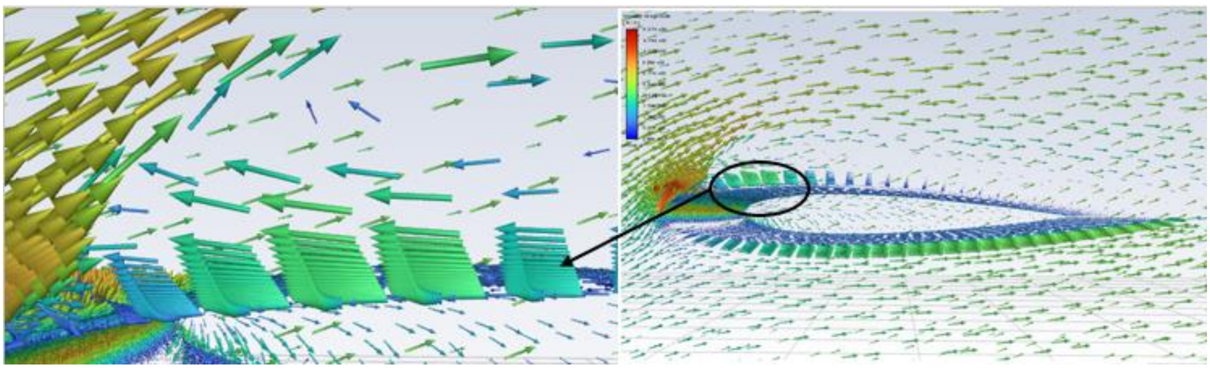

Figure 4:Zoomed in Velocity vector showing reverse flow at 15°AOA

In Figure 7, the reverse flow, at 15°AOA, begins to occur at a much closer position to the leading edge as compared to 10°AOA. From the overall observation at various AOAs, it can be concluded that the boundary layer separation is a function of Angle of Attack (AOA). The higher the angle of attack, the sooner boundary layer separation occurs on the upper wing surface.

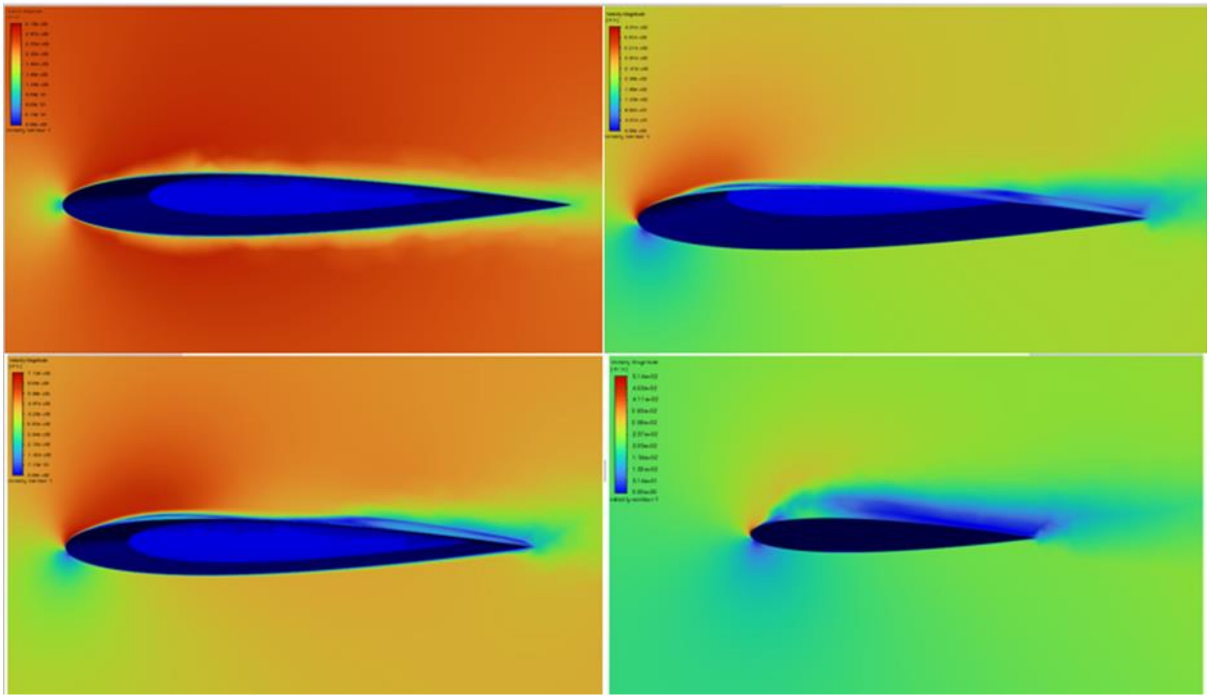

a)

Figure 5: Velocity contours at di b) **t AOA a)0° b)5° c)10° d)15°**

From the velocity contours in Figure 8, it can be seen that the stagnation point kept moving towards the lower leading edge as the air delivered to it kept introducing the wing to higher AOA. Additionally, at 0°AOA, there was no low velocity regions at the upper surface of the wing. But as the angle of attack increased, the low velocity regions became more evident especially at 15°AOA. These regions are equivalently high-pressure regions and are influenced by the occurrence boundary layer separation.

Experimental Results

The Experimental velocity at the test section was determined to be **1.98m/s.**

c)

d)

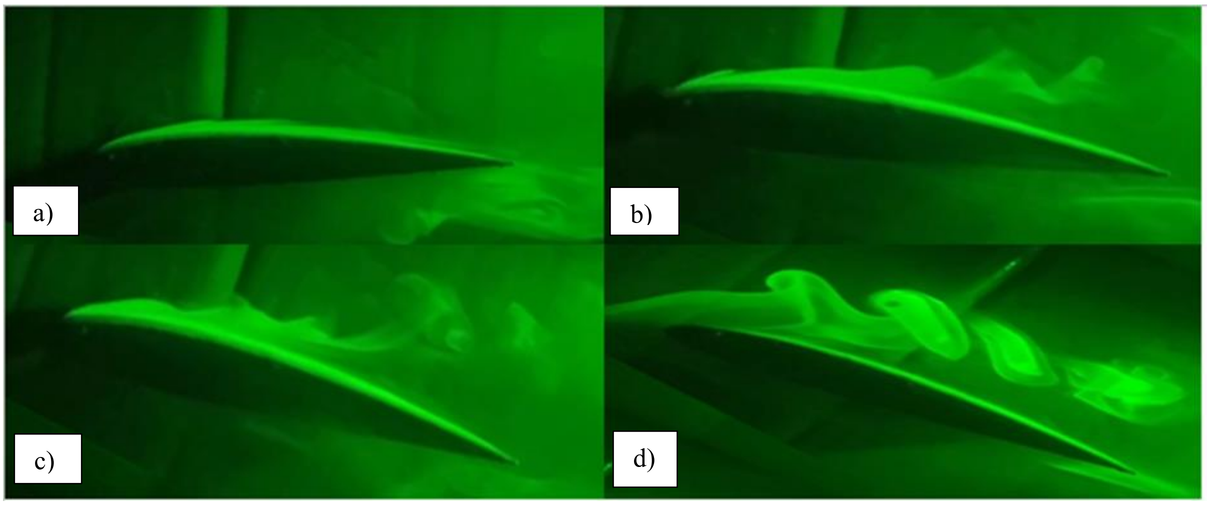

Figure 6: wing section in the test section at various AOA a)0°b)$5.^{\circ}$c)10°d)15°

Figure 7: Visualized flow in wind tunnel

At 0° AOA, the boundary layer over the wing is laminar throughout the wing surface with no separation point. As the AOA is increased to 5°AOA, the laminar boundary layer, turbulent one and boundary layer point of separation are clearly visible. Furthermore, increasing the AOA to 10°, the boundary layer point of separation occurred at slightly upstream position on the wing surface as compared to the previous 5°AOA. Finally, increment up to 15 degrees AOA, the separation of the boundary layer occurred at a more upstream position as compared to the preceding AOA. And a repeating pattern of swirling vortices are seen creating Von Karman vortex street.

4.3. Analytical Result

The analytical velocity at the test section is determined to be **2.19m/s.**

5. Validation

The laser beam apparatus constructed requires a means of determining how accurate and reliable it is, as an instrument. For that reason, the velocity at the test section is determined analytically, by theoretical calculations using mass flow rate equation and experimentally by use of a mini anemometer. The values determined are computed to find the percentage error, taking analytical velocity as reference. This percentage error was calculated to be 9.59%.

6. Conclusion

In this paper a designed and implemented laser beam apparatus for flow visualization was executed. The apparatus setup was for observing and analyzing the flow patterns which is a crucial technique in fluid mechanics for understanding complex flow behaviors. With the laser source in conjunction with smoke form the generator as tracer particles and a lens, the required illumination was achieved to properly observe the vortex formations as the flow passed over the airfoil in the test section. The key to understanding this flow was on the base of boundary layer attachment and detachment to the airfoil body being tested in the test section, which was captured, and shown in the pictures earlier. Considering the objectives outlined, the vortex formations, boundary layer and patterned were observed and analyzed which curbs the success of the work.

7. Acknowldgement

The successful completion of this work could not have been brought to fruition without the prolific guidance of Dr. Dharmahinder Singh Chand, Head of the Department of Aerospace Engineering at Chandigarh University. His rich knowledge in the field helped us in understanding complicated concepts. His belief and encouragement lead the team to this very moment. Thanks, is also rendered to the aerospace engineering laboratory technician for their continuous cooperation for the experimentation

8. References

[1] Kamaruddin, N. M., & Ismail, A. T. (2020). Development of a flow visualization technique in wind tunnel for hydrokinetic turbine application. Renewable Energy, 160, 1234–1245. https://doi.org/10.1016/j.renene.2020.07.108

[2] Kumbhare, S., & Rao, H. J. (2023). Design of a low-speed smoke visualization wind tunnel. Journal of Aerospace Engineering, 36(2), 04023012. https://doi.org/10.1061/(ASCE)AS.1943-5525.0001489

[3] Sayed, A., Abhishek, E., Hasan, S., Reddy, K. S., Chandrasekhar, P., & Chand, D. S. (2023). Flow visualization by laser sheet in a smoke-tunnel. Journal of Fluids Engineering, 145(5), 051301. https://doi.org/10.1115/1.4056725

[4] Rodríguez-Sevillano, Á. A. (2023). Exploring the effectiveness of visualization techniques for NACA symmetric airfoils at extremely low Reynolds numbers. Fluids, 8(7), 207. https://doi.org/10.3390/fluids8070207

[5] Crimaldi, J. P., & Knight, D. W. (2023). A laser-based flow visualization system for fluid mechanics instruction. Journal of Fluids Engineering, 145(3), 031301. https://doi.org/10.1115/1.4055986

[6] Mejia, K. M., & Jorgens, C. J. (2023). Conceptual design of a laser light sheet flow visualization system for a pressurized, low speed wind tunnel. Journal of Aircraft, 60(4), 1234–1245. https://doi.org/10.2514/1.C037353

[7] Reinath, M., & Ross, J. (2023). A laser-sheet flow visualization technique for the large wind tunnels of the National Full-Scale Aerodynamics Complex. NASA Technical Memorandum, TM-2023-12345, 1–15.

[8] Maresca, C., Berton, E., & Favier, D. (2023). Embedded LDV measurements in the boundary layer of moving walls. Experimental Thermal and Fluid Science, 145, 110987. https://doi.org/10.1016/j.expthermflusci.2023.110987

[9] Kikuchi, T. (2023). An apparatus for flow visualization by smoke in circular wind tunnel. Journal of Wind Engineering and Industrial Aerodynamics, 230, 105–115. https://doi.org/10.1016/j.jweia.2023.105432

[10] Dobin, N. (2023). Analysis of the air flow in the renovated test section of BSHC small wind tunnel. Journal of Wind Engineering and Industrial Aerodynamics, 235, 105432. https://doi.org/10.1016/j.jweia.2023.105432

[11] Flow visualisation by laser sheet in a smoke-tunnel. (2024). Journal of Mathematical Techniques and Computational Mathematics. https://doi.org/10.33140/jmtcm.03.01.03

[12] Cholemari, M. R., & Mathur, M. K. (2025). Quantitative smoke visualization: An optical field measurement technique for measuring scalar concentration using Mie scattering from smoke particles. Physics of Fluids. https://doi.org/10.1063/5.0247227

[13] Shamsuddin, M., & Kamaruddin, N. (2020). Design and development of a small-scale wind tunnel for flow visualization. IOP Conference Series: Materials Science and Engineering, 920(1), 012001. https://doi.org/10.1088/1757-899X/920/1/012001

[14] Aguilera, C., Sosa, J., Hyde, E. W., Miklosovic, D., & Kessler, D. A. (2023). Supersonic wind tunnel flow characterization using planar laser CO_2 Rayleigh scattering. Journal of Aircraft. https://doi.org/10.2514/1.C037243

[15] Ismail, A., & Kamaruddin, N. (2020). Development of a flow visualization technique in wind tunnel for hydrokinetic turbine application. IOP Conference Series: Materials Science and Engineering, 920(1), 012034. https://doi.org/10.1088/1757-899X/920/1/012034

[16] Rohlfs, L., Hastrich, L., Gothow, A., & Weiss, J. (2024). TUBflow – An open source application for digital postprocessing of oil film visualizations in wind tunnels. AIAA AVIATION Forum and ASCEND 2024. https://doi.org/10.2514/6.2024-4283

[17] Shamsuddin, M., & Kamaruddin, N. (2020). Design and development of a small-scale wind tunnel for flow visualization. IOP Conference Series: Materials Science and Engineering, 920(1), 012001. https://doi.org/10.1088/1757-899X/920/1/012001

[18] Flow visualisation by laser sheet in a smoke-tunnel. (2024). Journal of Mathematical Techniques and Computational Mathematics. https://doi.org/10.33140/jmtcm.03.01.03

[19] Castellani, F., Eltayesh, A., Natili, F., Tocci, T., Becchetti, M., Capponi, L., Astolfi, D., & Rossi, G. (2021). Wind flow characterisation over a PV module through URANS simulations and wind tunnel optical flow methods. Energies, 14(20), 6546. https://doi.org/10.3390/en14206546

9. Conflict of Interest

The author declares no competing conflict of interest.

10. Funding

No funding was issued for this research.